The effect of Gd addition on the kinetics of α₂→γ transformation in γ-TiAl based alloys

V.S. Sokolovsky [a,*], N.D. Stepanov [a], S.V. Zherebtsov [a], E.I. Volokitina [a], P.V. Panin [b], N. A. Nochovnaya [b], S.D. Kaloshkin [c], G.A. Salishchev [a]

[a] *Belgorod State University, 85 Pobeda Str, 308015, Belgorod, Russian Federation*
[b] *Federal State Unitary Enterprise "All-Russian Scientific Research Institute of Aviation Materials", 17 Radio Str, 105005, Moscow, Russian Federation*
[c] *National University of Science and Technology "MISIS", Leninsky pr. 4, 119049, Moscow, Russia*

ARTICLE INFO

ABSTRACT

The effect of Gd on the formation of a lamellar structure during ageing of quenched γ-TiAl based alloys was studied. Ti-47.1Al-1.8Nb-0.5Zr-0.3V-0.001Gd (0.001Gd) and Ti-46.9Al-1.6Nb-0.5Zr-0.5V-0.03Gd (0.03Gd) alloys were quenched from the alpha-phase field and aged at 400–800 °C. After quenching, a small amount of Gd_2TiO_5 particles was found in both alloys. Grain boundary segregation of Gd in the 0.03Gd alloy quenched from the alpha-phase field was detected. The α₂→γ transformation kinetics with the formation of γ lamellae was found to be noticeably faster in the 0.001Gd alloy. In addition, an increase in the Gd percentage led to a reduction of the interlamellar spacing for all ageing conditions. The effect of Gd on surface energy and diffusion rate are discussed.

1. Introduction

Gamma titanium aluminide based alloys are promising structural materials which can be used for gas turbine blades manufacturing [1]. However, oxygen impurities can deteriorate the structure and properties of these alloys substantially [2]. One of the ways to reduce the level of harmful impurities is micro-alloying with rare earth elements (REE). Since REE are active getters which decrease the content of dissolved oxygen, REE doping has a positive effect on mechanical properties of gamma titanium aluminide based alloys [2]. Because of extremely small solubility in both the γ- and α₂-phases an addition of REE leads to the formation of oxides and aluminides particles [3].

Another effect of REE containing particles and possibly REE themselves can be associated with a decrease both in the colony/grain size and interlamellar spacing [4–6]. For example [5], a study of the Ti–47Al binary alloy (at. %) doped with Y showed that the grain size decreases gradually from 1200 to 60 μm with Y addition to 1.0 at. %. The interlamellar spacing ranges were from 1.3 μm in Ti-47A1 alloy to 0.18 μm in Ti-47A1-1.0 Y alloy. It was noted that at an optimal concentration of Y 0.3–0.5 at. %, the highest values of strength and ductility were observed.

The use of high-temperature heat treatment can result in the dissolution of REE - based particles [7], thereby allowing to control their size and distribution. However, REE (being surface-active elements) often form segregations at the boundaries and influence on the phase transformations in the solid state due to the corresponding surface energy reduction [8]. In addition, REE can change diffusivity [9], which will obviously influence the kinetics of phase transformations. The influence on the phase transformations kinetics is due a combined effect of i) increased rate of the γ phase nucleation and ii) decreasing in the lateral growth rate of α₂/γ lamella. Meanwhile this effect of REE has not been investigated so far.

In this paper the effect of Gd on the α₂→γ transformation kinetics during ageing of quenched gamma titanium aluminide based alloys with different Gd content was evaluated.

2. Materials and methods

The ingots measured approximately $25 \times 25 \times 25$ mm³ were produced by vacuum arc melting. The actual chemical compositions of the Ti–Al–Nb–Zr–V–Gd alloys measured by SEM-based EDS are shown in Table 1. For the sake of simplicity, hereafter these alloys are referred to as 0.03 Gd and 0.001 Gd. Although there is also a slight difference in the Al, Nb and V content between the alloys, the influence of these variations on the formation of a lamellar structure is minimal.

Table 1
Chemical composition of the program alloys, in at. %.

	Ti	Al	Nb	Zr	V	Gd
Alloy 1	Bal.	46.9	1.6	0.5	0.5	0.03
Alloy 2	Bal.	47.1	1.8	0.5	0.3	0.001

Dilatometry (Model DIL 402 C, Netzsch-Gerätebau GmbH, specimens measured $4 \times 4 \times 20$ mm^3) and differential scanning calorimetry (DSC) (SDT Q600 TA Instruments, specimens measured $4 \times 4 \times 1.5$ mm^3) analysis were used to determine temperatures of phase transformations. Specimens were cut from the as-cast ingot using an electric discharge machine and then mechanically polished. The measurements were carried out in the temperature range of 25–1450 °C in Ar atmosphere.

Specimens used for heat treatment (measured $10 \times 10 \times 20$ mm^3) were sealed in quartz capsules contained also titanium chips as a getter and filled with pure argon. The samples were solute treated at T = 1350 °C (alpha phase field) for 2 h with subsequent water quenching. No cracks or noticeable microstructure gradients were observed in the quenched samples. The quenched samples were then aged at 400, 500,

600, 700 or 800 °C for 5, 10 or 60 min; after the ageing the specimens were water quenched.

The microstructure was examined using scanning (SEM) and transmission (TEM) electron microscopy. Specimens for SEM analysis were mechanically polished. SEM investigations were carried out using a FEI Quanta 600 FEG (field emission gun) microscope in a backscattered electron (BSE) mode; the microscope was equipped with an energy-dispersive (EDS) detector. Samples for TEM analysis were first mechanically ground to ~ 100 μm thickness and then electro-polished in a mixture of 5% perchloric acid, 35% butanol and 60% methanol at 27 V and −32 °C using a twin-jet TenuPol-5 Struers. TEM investigations were carried out using a JEOL JEM - 2100 microscope operated at 200 kV and equipped with an EDS detector. Phase diagrams for the Ti–XAl-1.6Nb-0.5Zr-0.5V and Ti–XAl-1.8Nb-0.5Zr-0.3V (X = 35–50) alloys were calculated using a Thermo-Calc software (version TCW5, database TTTIAL). Note that the TTTIAL database does not include Gd and therefore it has been omitted from the thermodynamic calculations.
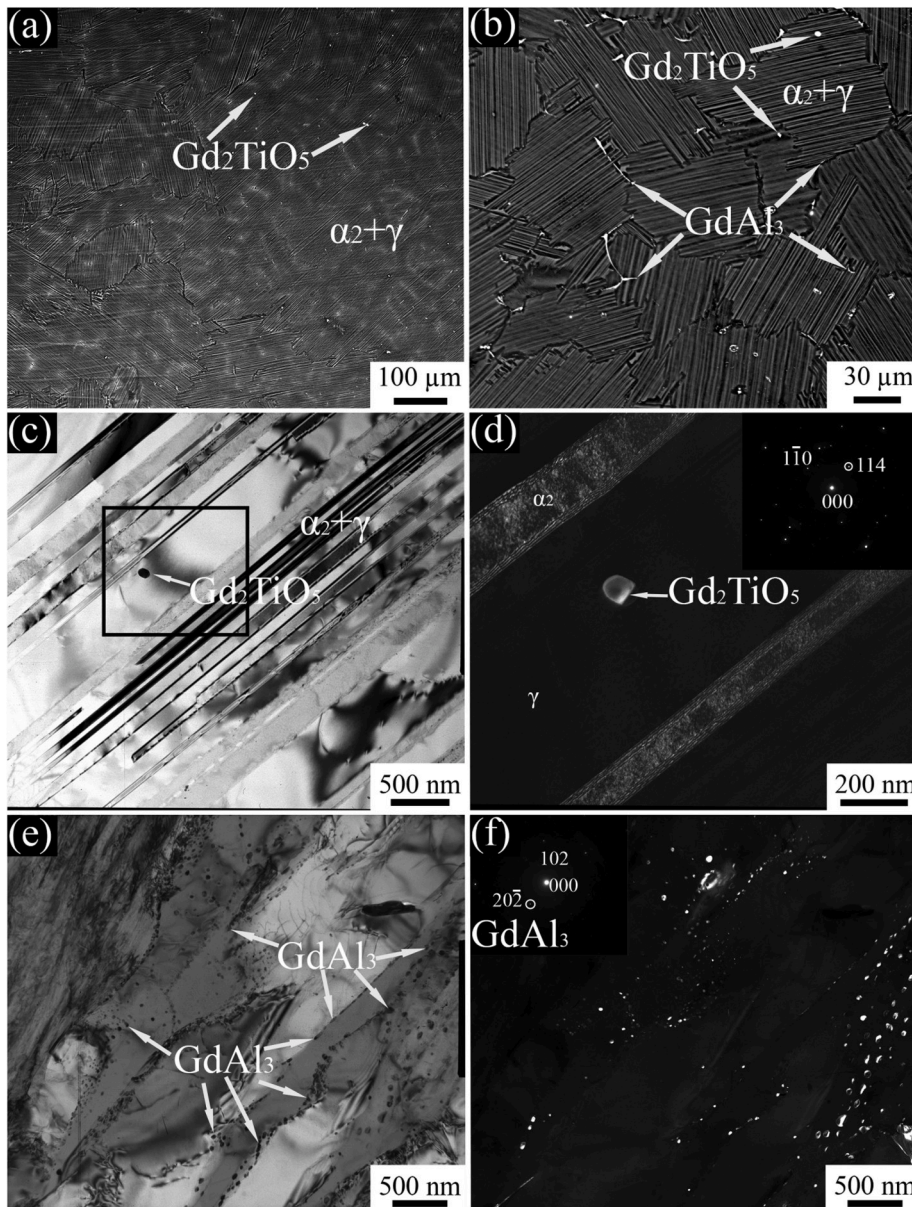
Fig. 1. Microstructure of the as-cast 0.03 Gd alloy: a) an overview at low magnification; b) the Gd$_2$TiO$_5$ and GdAl$_3$ particles at higher magnification; c) a particle of the Gd$_2$TiO$_5$ phase inside a α$_2$+γ colony (bright field); d) a dark-field image of the Gd$_2$TiO$_5$ phase particle and the corresponding selected area electron diffraction (SAED) pattern (inserted); e) nearly equiaxed GdAl$_3$ particles at boundaries between α$_2$+γ colonies (bright field), f) a dark-field image of the GdAl$_3$ phase particles. (a–b) SEM-BSE images; (c–f) TEM images.
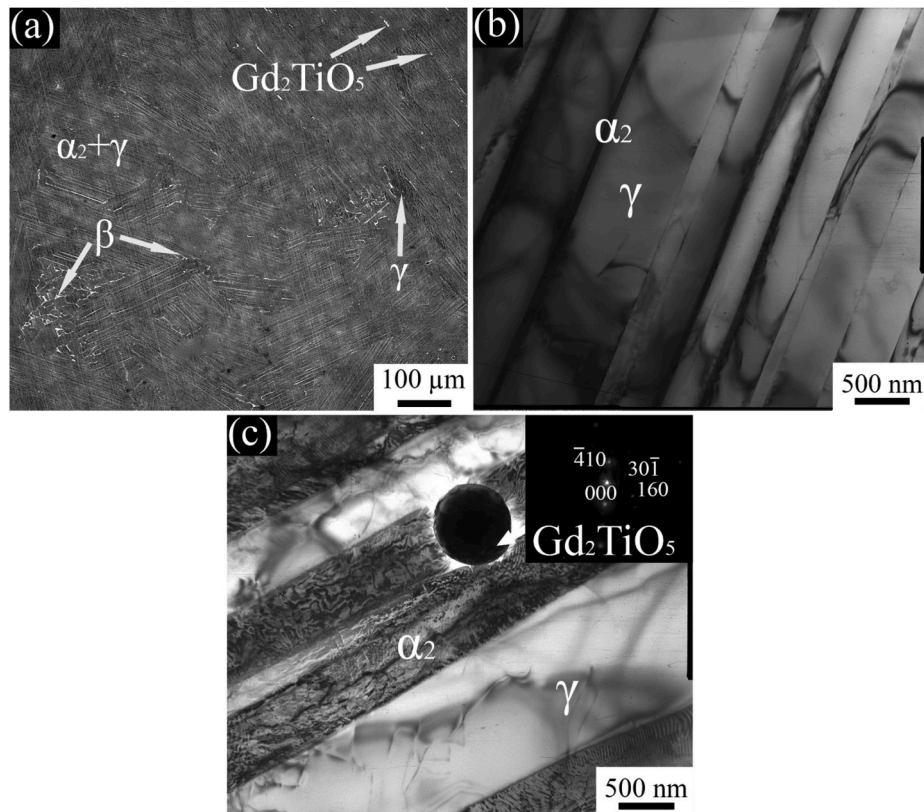
Fig. 2. Microstructure of the as-cast 0.001Gd alloy: a) an overview at low magnification; b) an $\alpha_2+\gamma$ lamellar structure; c) a Gd_2TiO_5 phase particle inside an $\alpha_2+\gamma$ colony and the corresponding SAED pattern; (a) SEM-BSE images; (b–c) TEM images.

3. Results

3.1. As-cast condition

Microstructure of the as-cast 0.03 Gd alloy consisted mainly of $\alpha_2+\gamma$ lamellar colonies; Gd-rich particles were located both within and at the boundaries of the colonies (Fig. 1). The particles were identified as Gd_2TiO_5 (Fig. 1a–d) or $GdAl_3$ (Fig. 1b, e, f). The size and volume fraction of the Gd-rich particles were 0.1–4.5 μm and 1.3%, respectively. The particles were heterogeneously distributed (Fig. 1). The $GdAl_3$ phase particles predominantly located at boundaries (Fig. 1b, e, f) had both a plate-like (Fig. 1b) and spherical morphology (Fig. 1e and f). They were sometimes observed in clusters (Fig. 1e and f). The volume fraction of the $GdAl_3$ phase was ~0.5%. The Gd_2TiO_5 particles were equiaxed and distributed more homogeneously in the microstructure (Fig. 1a–d). The

volume fraction of the Gd_2TiO_5 phase was ~0.8%. The size of the $\alpha_2+\gamma$ colonies was approximately 150 μm (Fig. 1a and b) with the average interlamellar spacing (λ) of 230 nm (Fig. 1c and d).

The microstructure of the as-cast 0.001Gd alloy mostly consisted of $\alpha_2+\gamma$ lamellae colonies with separate particles of γ and β phases. In addition, homogeneously distributed Gd_2TiO_5 particles measured 0.5–8.5 μm with a volume fraction of ~0.1% can be found (Fig. 2). The lamellar colonies' size was approximately 260 μm (Fig. 2a) with the average interlamellar spacing of 450 nm (Fig. 2b and c).

3.2. Quenched condition

The $\alpha \rightarrow \alpha+\gamma$ phase transformation temperature in the 0.03 Gd alloy was determined by DSC or dilatometry to be 1327 °C or 1330°C, respectively. In the 0.001 Gd alloy the phase transformation
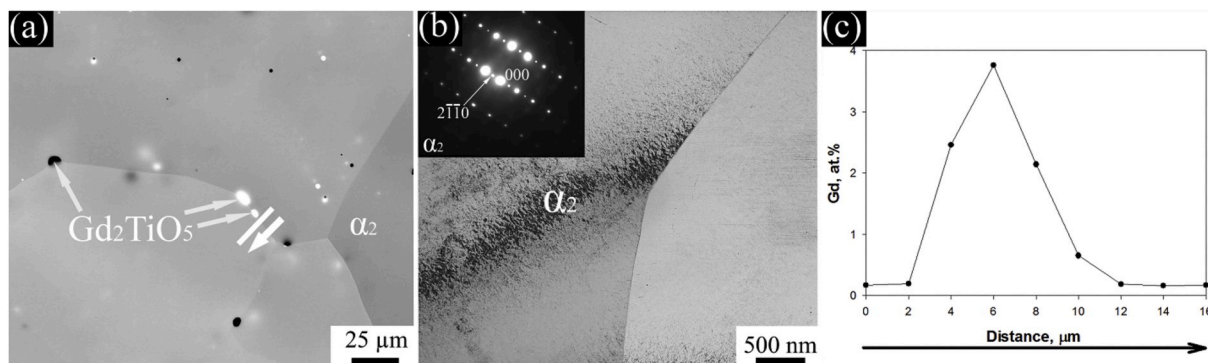
Fig. 3. Microstructure of the 0.03 Gd alloy after quenching from the α-phase field: a) SEM-BSE image; a white line and arrow across a border indicates the area and direction of Gd distribution measurement (the result is shown in Fig. 3c); b) TEM bright-field image of the α_2 phase with the corresponding SAED pattern; c) distribution of Gd across the grain boundary in Fig. 3a.
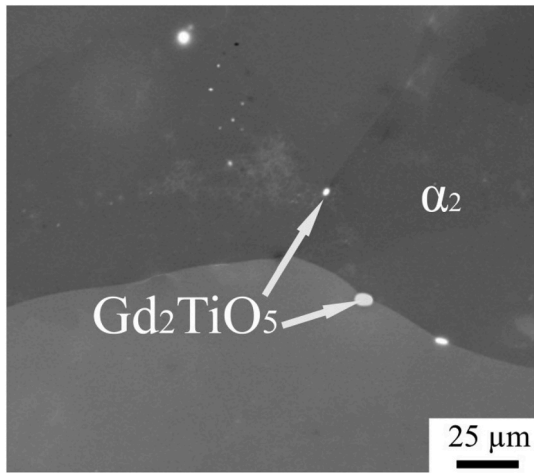
Fig. 4. SEM-BSE image of the 0.001 Gd alloy microstructure after quenching from the α-phase field.

temperatures were quite similar: 1330 °C and 1334 °C per DSC and dilatometry, respectively. Therefore, both the alloys were solution treated at 1350 °C. Note that T = 1350°C is also above the solvus

temperature of the GdAl$_3$ phase [10]. Fig. 3 shows an almost entirely single α$_2$ phase in the 0.03 Gd alloy after soaking in the alpha-phase field. Ordering of the metastable α-phase during quenching from the alpha phase field was expected to result in the formation of the α$_2$-phase [1,11]. TEM bright-field image with the corresponding SAED pattern (Fig. 3b) confirmed the formation of the α2 phase. After quenching, GdAl$_3$ particles were not detected however a small amount (~0.8 vol %) of the Gd-rich oxides survived (Fig. 3a). SEM-EDS data demonstrates a 20-times increase in the gadolinium content across a grain boundary (Fig. 3a, c), thus suggesting Gd segregation at the boundaries.

The microstructure of the 0.001 Gd alloy after solute treatment at 1350 °C (α-phase field) for 2 h consisted of equiaxed α$_2$ grains (Fig. 4). The size and volume fraction of the Gd$_2$TiO$_5$ particles after quenching did not change compared with the as-cast condition (Fig. 4).

3.3. Effect of ageing

The effect of temperature and time of ageing on the interlamellar spacing (λ) in the 0.03 Gd alloy is shown in Fig. 5. An isolated γ-phase lamella of 50–1000 nm in length inside a grain of the α$_2$-phase was observed after ageing of the alloy at T = 400 °C for 5 min (Fig. 5a). An increase in the soak time to 10 min led to a complete α$_2$→γ transformation (Fig. 5b) without any noticeable changes after 60 min treatment (Fig. 5c). Ageing at higher temperatures (500–600°C) resulted in a
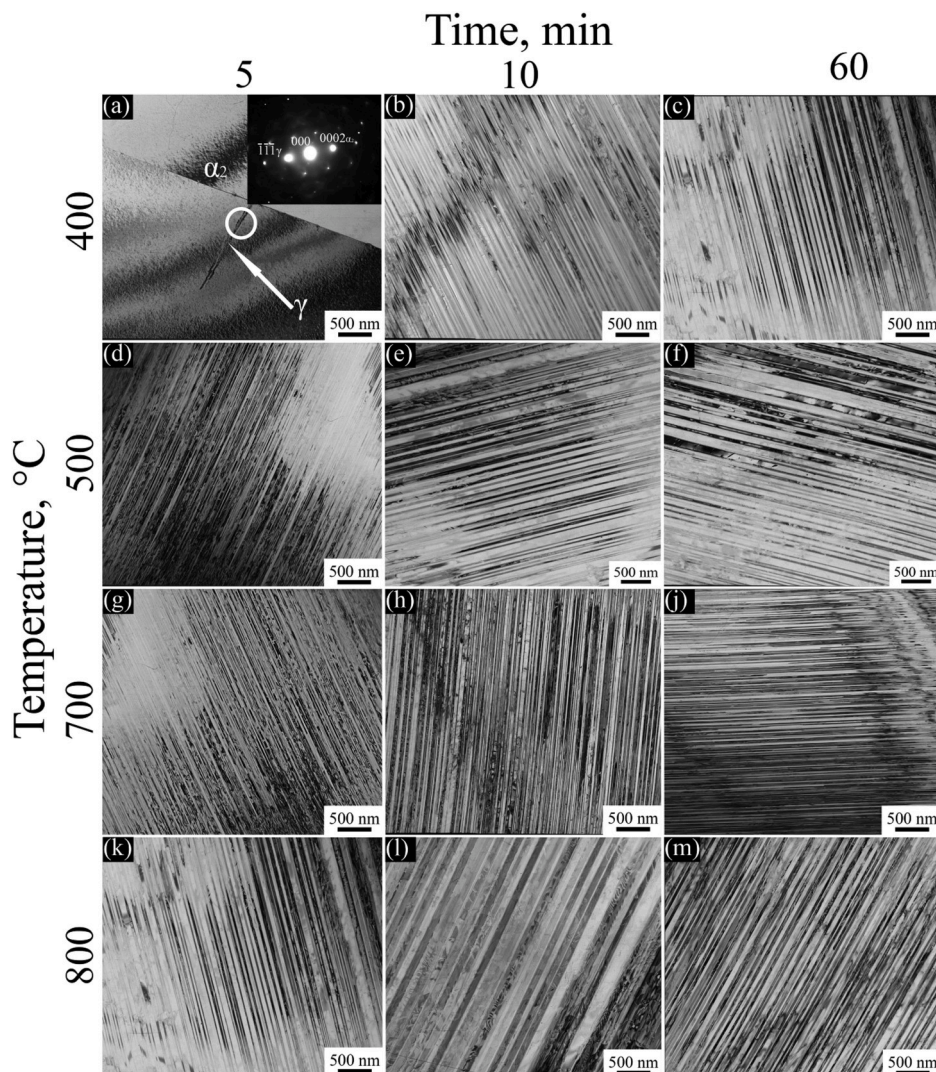

Fig. 5. TEM bright-field images of the 0.03 Gd alloy after ageing at 400–800C for 5, 10 and 60 min. SAED pattern in Fig. 5a is shown for the γ and α$_2$ phases.
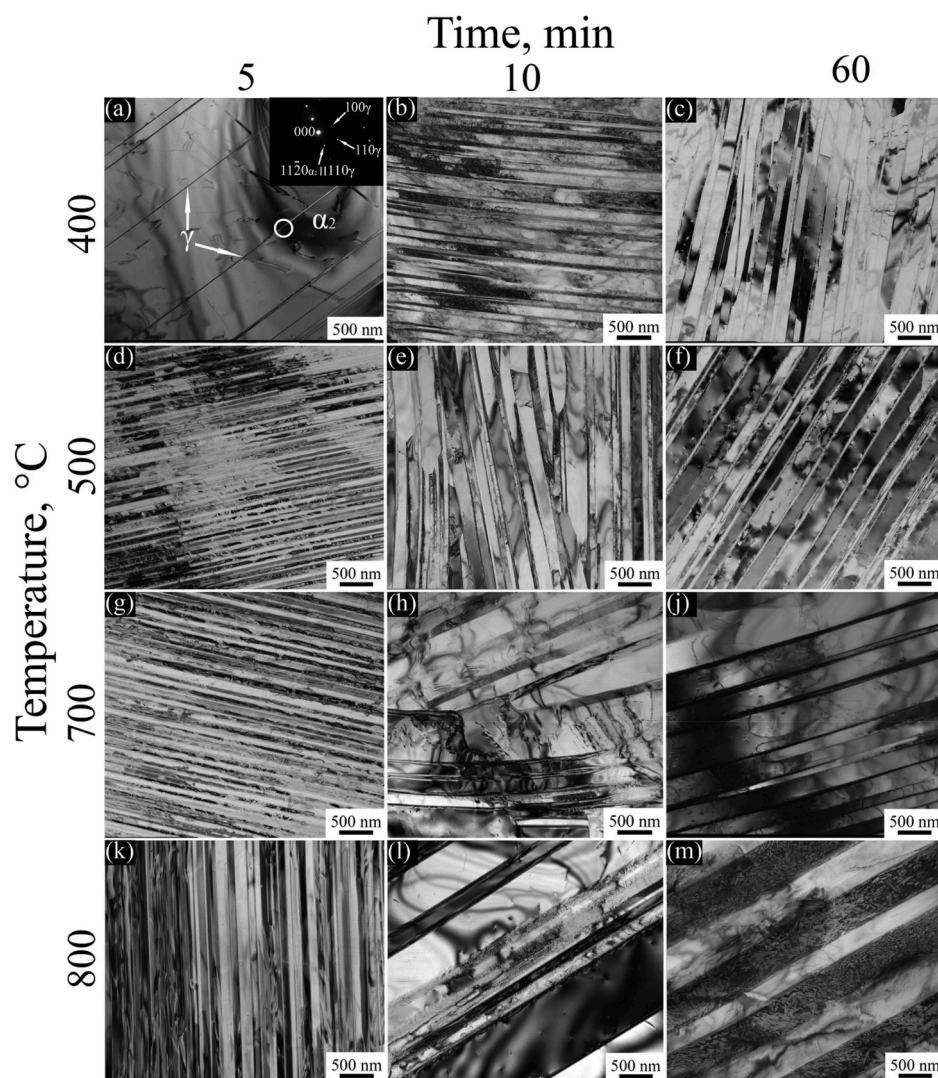
Fig. 6. TEM bright-field images of the 0.001 Gd alloy after ageing at 400–800C for 5, 10 and 60 min. SAED pattern in Fig. 5a is shown for the γ and α$_2$ phases.

complete filling of the α$_2$ phase grains with the γ-phase lamellae already after 5 min soaking (Fig. 5d, g, k). An increase in the soaking time resulted mainly in some increase in the interlamellar spacing (Fig. 5e, f, h, j). A significantly higher interlamellar spacing was obtained after ageing at 800 °C, however, qualitatively the dependence of spacing on soaking time at 800°C was similar to that at lower temperatures.

The microstructure of the 0.001 Gd alloy after ageing (Fig. 6) was in general close to that in the 0.03 Gd alloy (Fig. 5). For example, after 5 min ageing only a limited number of γ lamellae in the α$_2$ matrix was found in the 0.001 Gd alloy (Fig. 6a) (however, the amount of the γ phase was much higher than in the 0.03 Gd alloy (Fig. 5a)). An increase in the ageing time and/or temperature led to the entirely lamellar α$_2$+γ microstructure. The interlamellar spacing also gradually increased with the annealing temperature and time (Fig. 7b, d), similarly to the 0.03 Gd alloy (Fig. 7a, c). It should be noted, however, that the increase in the interlamellar spacing with temperature in the 0.001 Gd alloy was much more gradual than that in the 0.03 Gd alloy where significant growth was found at 800 °C only. Besides, the absolute values of λ after the same processing were ~2–3 times higher in the alloy with the lower amount of Gd (Fig. 7). Note also that new Gd-rich phase particles were not formed in both alloys during the ageing (in attrition to those which were seen in the as-quenched condition).

4. Discussion

The obtained data elucidate the effect Gd on the α$_2$→γ transformation kinetics (Figs. 5–7) and some structural parameters in two gamma titanium aluminide based alloys that worth detailed consideration. The major difference between the program alloys was the amount of Gd-rich phases in the as-cast and quenched conditions. The volume fraction of Gd-rich phases in 0.001 Gd and 0.03 Gd alloys was 0.1% and 1.5%, respectively. In the 0.03 Gd alloy the total volume fraction of the Gd-rich phases included 0.8% of the Gd$_2$TiO$_5$ phase and 0.5% of the GdAl$_3$ phase. After annealing in the α-phase field the volume fraction of the Gd$_2$TiO$_5$ phase in the 0.001 Gd and 0.03 Gd alloys was 0.1% and 0.8%, respectively. It should be noted that the as-cast 0.001Gd alloy (Fig. 2a) contained laths of the metastable β-phase which was not predicted by the calculated phase diagram (Fig. 8b). Probably, the β-laths formation was caused by non-equilibrium crystallization. However, it was not found in 0.03Gd alloy.

The alloys contained also slightly different amounts of Nb, Zr, and V (Table 1). Since the content of these elements can have some effect on phase transformations, it is interesting to clarify the influence of these variations in chemistry on phase stability in the alloys. For example, the effect of Nb on the interlamellar spacing in a binary Ti–45Al alloy [12] was ~30% (from 270 to 350 nm) for an increase in the Nb content from 0 to 10 at. %. The influence of V (which belongs to the same group of
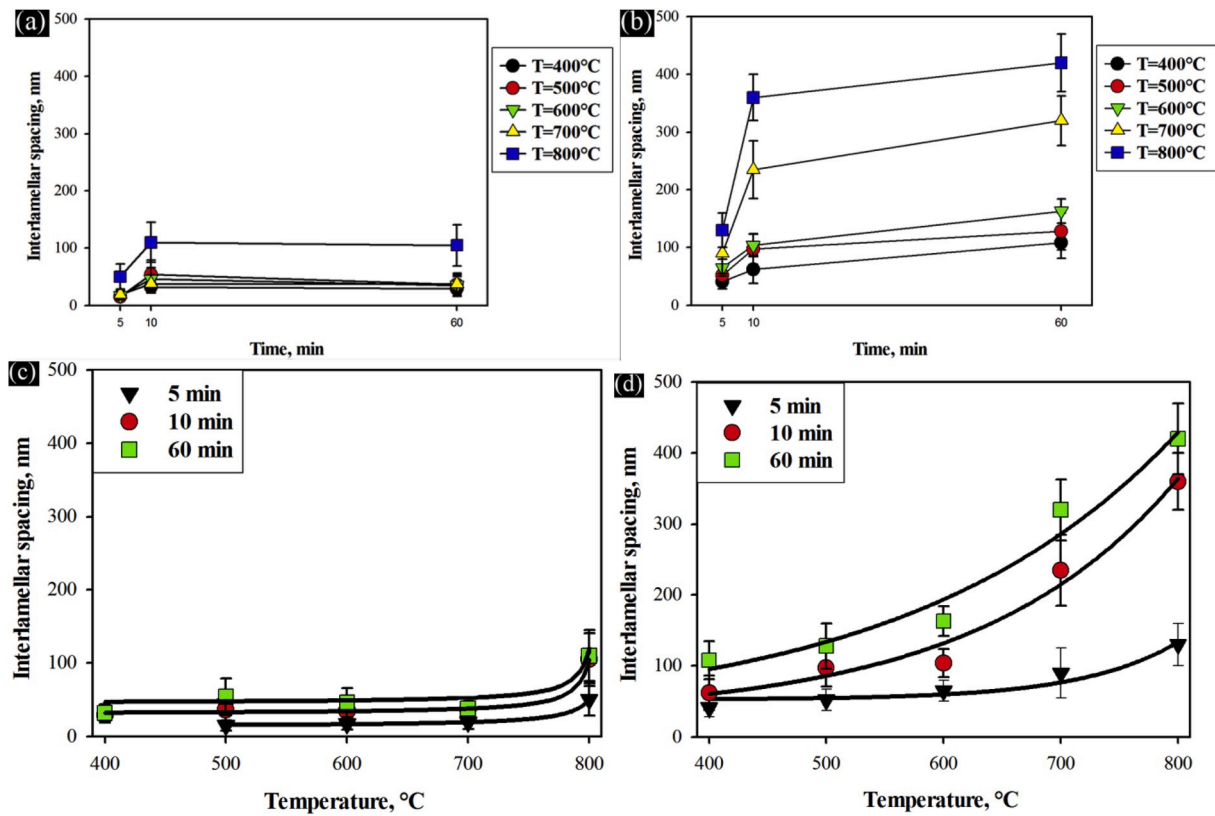
Fig. 7. Interlamellar spacing (λ) as a function of (a, b) soak time at different temperatures or (c, d) temperature at different soak times; (a, c) - 0.03 Gd alloy, (b, d) - 0.001 Gd alloy.
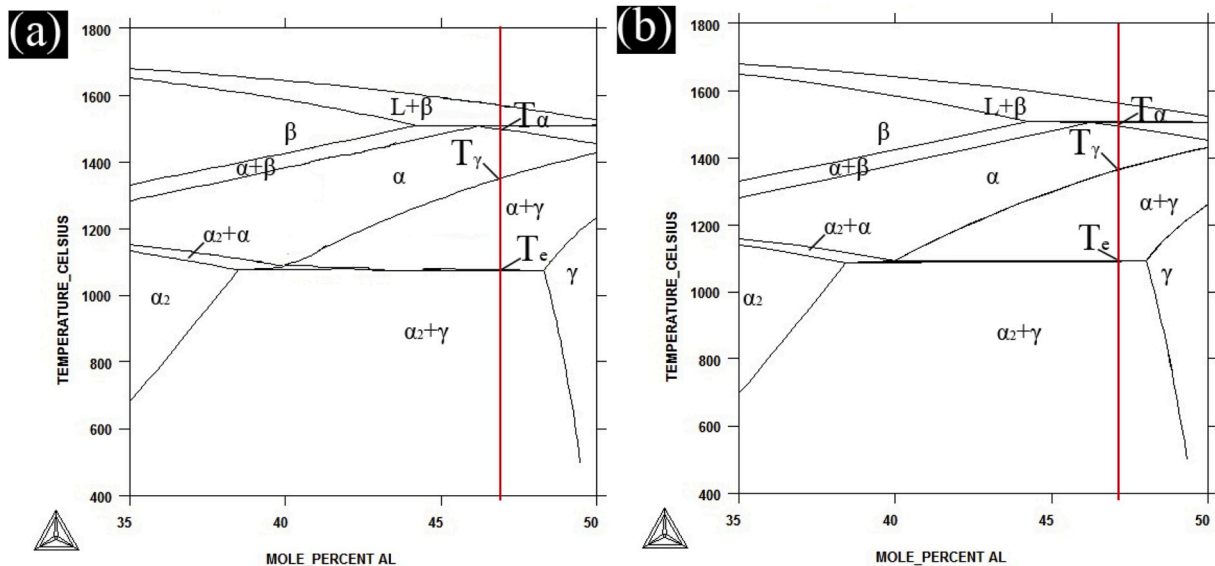

Fig. 8. Phase diagrams for the Ti–Al-1.6Nb-0.5Zr-0.5V (a) and Ti–Al-1.8Nb-0.5Zr-0.3V (b) alloys calculated by the Thermo-Calc software.

elements in the periodic table) was similar. Since the changes in the concentrations of these elements in the alloys are oppositely directed, the overall effect of this factor can be considered insignificant. In addition, variations in the chemical composition does not affect significantly elastic modulus thereby confirming a small effect of the chemical mismatch on the properties of the alloys; for example in Ref. [13] an increase in the content of Nb in Ti–25Al-xNb alloys from 4.9% to 20.3% decreased Young's modulus from 133 to only 128 GPa (~3.7%).

To get more detailed information on possible effect of chemical

composition variations on the phases in the alloys, we have produced corresponding equilibrium phase diagrams. Phase diagrams were constructed for different concentrations of Nb, Zr and V (1.8 or 1.6 at. % Nb in the 0.03 Gd or 0.001 Gd alloys, respectively; 0.5/0.5 at. % Zr, and 0.3/0.5 at. % V, respectively) and variable percentages of Al in the range 35.0–50.0 at. % using the Thermo-Calc software (Fig. 8, Table 2). Note that the available commercial thermodynamic database for TiAl-based alloys (TTTIAL) does not include Gd which therefore was excluded from the consideration. The sequence of the phases which form in the

Table 2

The calculated temperatures of the phase transformations in Ti-46.9Al-1.6Nb-0.5Zr-0.5V and Ti–47.1Al-1.8Nb-0.5Zr-0.3V alloys and corresponding experimental results for 0.03Gd and 0.001 Gd alloys.

Method	Phase transformation temperature, °C			
	Ti-46.9Al-1.6Nb-0.5Zr-0.5V/ 0.03 Gd		Ti–47.1Al-1.8Nb-0.5Zr-0.3V/ 0.001Gd	
	T_e	T_γ	T_e	T_γ
Calculated	1086–1097	1353	1090–1100	1368
DSC	1152–1184	1327	1148–1182	1330
Dilatometry	1163–1200	1330	1149–1192	1334

alloys during crystallization included the β, α, γ, and α_2 phases. The solvus temperatures of these phases were denoted as T_β, T_α and T_γ, respectively. The eutectoid reaction temperature at which the $\alpha \to \alpha_2 + \gamma$ transformation occurred was denoted as T_e.

Table 2 also contains phase transformation temperatures measured using both by DSC and dilatometry method. A comparison of the calculated and experimental data shows somewhat higher phase transformations temperatures obtained by the Thermo-Calc software. Note that some difference between measured and predicted temperatures of phase transformations for different γ-TiAl based alloys has been already reported earlier [14,15]. Nevertheless, reasonable agreement between the calculations and experiments was observed. Also, the calculated values for the two alloys were very close, which suggests that variations in Nb, Zr, and V are unlikely to affect the phase transformation temperatures considerably.

Besides, experimental data (i.e. DSC and dilatometry) showed very close values of T_e and T_γ in the alloys (Table 2). Therefore, Gd most probably does not affect the $\alpha \to \gamma$ and $\alpha \to \alpha_2 + \gamma$ transformation temperatures in the examined alloys. This assumption is in reasonable agreement with the observed microstructures, where almost identical phases were found in both alloys (Figs. 1–8).

Although after ageing the alloys were composed of the same α_2 and γ phases, a significant effect of Gd on the kinetics of $\alpha_2 \to \gamma$ transformation was revealed. An increase in the Gd content tended to retard the $\alpha_2 \to \gamma$ transformation kinetics. After ageing at T = 400 °C for τ = 5 min microstructure of the 0.03 Gd alloy consisted of individual lamellae of the γ-phase in grains of the metastable α_2-phase (Fig. 5a). Meanwhile in the 0.001 Gd doped alloy the number of the γ-laths was considerably greater (Fig. 6a). The thickness of the γ-phase lamellae was also different: 14 and 40 nm in the 0.03 Gd and 0.001 Gd alloys, respectively. The interlamellar spacing as a function of ageing temperature and soak time was not similar for the alloys with different content of Gd (Fig. 7). The greater amount of Gd reduced interlamellar spacing in all ageing conditions; however a noticeable increase in the interlamellar spacing in the 0.03 Gd alloy was noted at 700 °C, whereas in the 0.001 Gd alloy the onset of this increase occurred at 600 °C.

In γ-TiAl based alloys the formation of the γ phase in the metastable α_2 is associated with lattice shear [13]. However for the formation of the gamma phase nucleus and their growth a local enrichment with aluminum is necessary that requires activation of diffusion processes. The dissolution of the $GdAl_3$ particles during the solution treatment led to the redistribution of Gd along grain boundaries (Fig. 3) that can change the surface energy of grain boundaries and grain-boundary diffusion. Therefore it can be assumed that REE, which have low solubility in metals [16], in particular in titanium [17], are located in the boundary, thereby reducing the level of surface energy [6] and, consequently, facilitating the formation of new phases [18]. However, the obtained result showed retardation of the $\alpha_2 \to \gamma$ transformation. Most likely the Gd atoms at grain boundaries inhibit diffusion of Al thereby preventing another important condition for the transformation – gathering of sufficient amount of Al for the γ-phase formation. This conclusion is in agreement with a slight increase in the γ-phase lamellae thickness during ageing (Figs. 6 and 7).

Thus, the main effect of Gd on the $\alpha_2 \to \gamma$ phase transformation can be ascribed to the hindering of the γ-phase nuclei formation due to an inhibition of diffusion and necessity of increased time/temperature for the attaining of a required concentration of Al. This leads to some retardation of the transformation kinetics, an increase in the nucleation rate of a new phase, and slower growth of particles during ageing. This was expressed earlier as an assumption in the work [6]. However, as it was observed in γ-TiAl-based alloys [19,20], diffusion becomes more active at temperatures 700–800 °C resulting in an increase in the interlamellar spacing in the 0.03Gd alloy due to the Gd atoms redistribution.

5. Conclusions

1. The structure of the as-cast and quenched from 1350 °C Ti-47.1Al-1.8Nb-0.5Zr-0.3V-0.001Gd and Ti-46.9Al-1.6Nb-0.5Zr-0.5V-0.03Gd alloys was investigated. Both program alloys had quite a similar structure in the as-cast condition mostly composed of $\alpha_2 + \gamma$ lamellar mixture. In the 0.03Gd alloy, 1.3% of Gr-rich Gd_2TiO_5 or $GdAl_3$ particles were found, whereas in 0.001Gd alloy only 0.1% of Gd_2TiO_5 was observed. After quenching from 1350 °C, both alloys had almost entirely α_2 phase structure, however, Gd_2TiO_5 particles remained intact. The similar phase composition of the alloys agrees with the Thermo-Calc predictions.
2. After quenching, the alloys were aged at 400–800 °C to produce γ lamellae in the α_2 matrix. The thickness of the γ lamellae in the 0.03 Gd alloy was noticeably lower than in the 0.001 Gd alloy. Also, after ageing at 400 °C for 5 min much smaller amount of γ lamellae was found in the 0.03 Gd alloy. The retardation of $\alpha_2 \to \gamma$ phase transformation kinetics was attributed to inhibition of diffusion in the alloy with higher Gd percentage.

CRediT authorship contribution statement

V.S. Sokolovsky: Writing - original draft, Methodology, Investigation. **N.D. Stepanov:** Writing - review & editing. **S.V. Zherebtsov:** Writing - review & editing. **E.I. Volokitina:** Investigation. **P.V. Panin:** Resources, Methodology. **N.A. Nochovnaya:** Resources. **S.D. Kaloshkin:** Methodology. **G.A. Salishchev:** Conceptualization, Supervision.

Acknowledgment

Appendix A. Supplementary data

Supplementary data to this article can be found online at https://doi.org/10.1016/j.intermet.2020.106759.

References

[1] F. Appel, J.D.H. Paul, M. Oehring, Gamma Titanium Aluminide Alloys: Science and Technology, Wiley-VCH, Weinheim, 2011.

[2] H. Liu, Z. Li, F. Gao, Y. Liu, Q. Wang, High tensile ductility and strength in the Ti-42Al-6V-1Cr alloy, J. Alloys Compd. 698 (2017) 898–905, https://doi.org/10.1016/j.jallcom.2016.12.306.

[3] C. Liu, K. Xia, W. Li, The comparison of effects of four rare earth elements additions on structures and grain sizes of Ti-44Al alloy, J. Mater. Sci. 37 (2002) 1515–1522, https://doi.org/10.1023/A:1014900325485.

[4] Y. Wu, S.K. Hwang, The effect of yttrium on microstructure and dislocation behavior of elemental powder metallurgy processed TiAl-based intermetallics, Mater. Lett. 58 (2004) 2067–2072, https://doi.org/10.1016/j.matlet.2003.12.036.

[5] F. Kong, Z. Chen, J. Tian, Y. Chen, J. Jia, Effect of rare earth on microstructure of γ-TiAl intermetallics, J. Rare Earths 21 (2003) 163–166.

[6] B. Li, F. Kong, Y. Chen, Effect of yttrium addition on microstructures and room temperature tensile properties of Ti-47Al alloy, J. Rare Earths 24 (2006) 352–356, https://doi.org/10.1016/S1002-0721(06)60123-3.

[7] J. Zhang, D. Feng, F. Yin, Some new aspects in developing TiAl based alloys as competitive high temperature materials, Adv. Mater. Res. 278 (2011) 557–562. www.scientific.net/AMR.278.557.

[8] Q. Zhang, T.W. Fan, L. Fu, B.Y. Tang, L.M. Peng, W.J. Ding, Ab-initio study of the effect of rare-earth elements on the stacking faults of Mg solid solutions, Intermetallics 29 (2012) 21–26, https://doi.org/10.1016/j.intermet.2012.04.015.

[9] T. Inoue, H. Matzke, Uranium self-diffusion in UC doped with Y, Zr, La or Ce, J. Nucl. Mater. 91 (1980) l–12, https://doi.org/10.1016/0022-3115(80)90026-4.

[10] L. Jin, Y.B. Kang, P. Chartrand, C.D. Fuerst, Thermodynamic evaluation and optimization of AlGd, AlTb, AlDy, AlHo and AlEr systems using a Modified Quasichemical Model for the liquid, Calphad Comput. Coupling Phase Diagrams Thermochem. 34 (2010) 456–466, https://doi.org/10.1016/j.calphad.2010.08.004.

[11] Y.Q. Sun, Surface relief and the displacive transformation to the lamellar microstructure in TiAl, Phil. Mag. Lett. 78 (1998) 297–305, https://doi.org/10.1080/095008398177878.

[12] Z.C. Liu, J.P. Lin, S.J. Li, G.L. Chen, Effects of Nb and Al on the microstructures and mechanical properties of high Nb containing TiAl base alloys, Intermetallics 10 (2002) 653–659, https://doi.org/10.1016/S0966-9795(02)00037-7.

[13] H. Warlimont, W. Martienssen, Springer Handbook of Materials Data, Springer International Publishing, 2018, https://doi.org/10.1007/978-3-319-69743-7.

[14] M. Schloffer, F. Iqbal, H. Gabrisch, E. Schwaighofer, F.P. Schimansky, S. Mayer, A. Stark, T. Lippmann, M. Göken, F. Pyczak, H. Clemens, Microstructure development and hardness of a powder metallurgical multi phase γ-TiAl based alloy, Intermetallics 22 (2012) 231–240, https://doi.org/10.1016/j.intermet.2011.11.015.

[15] A.V. Kuznetsov, V.S. Sokolovskii, G.A. Salishchev, N.A. Belov, N.A. Nochovnaya, Thermodynamic modeling and experimental study of phase transformations in alloys based on γ-tial, Met. Sci. Heat Treat. 58 (2016) 259–267, https://doi.org/10.1007/s11041-016-9999-2.

[16] W.G. Wilson, D.A.R. Kay, A. Vahed, Use of thermodynamics and phase equilibria to predict the behavior of the rare earth elements in steel, J Met 26 (1974) 14–23, https://doi.org/10.1007/BF03355873.

[17] H. Okamoto, Gd-Ti (Gadolinium-titanium), J. Phase Equilibria Diffus. 33 (2012) 422, https://doi.org/10.1007/s11669-012-0080-6.

[18] YaS. Umanskii, YuA. Skakov, Fizika Metallov. Atomnoe Stroenie Metallov I Splavov (Physics of Metals. Atomic Structure of Metals and Alloys), Atomizdat, Moscow, 1978.

[19] F. Appel, R. Wagner, Microstructure and deformation of two-phase γ-titanium aluminides, Mater. Sci. Eng. R Rep. 22 (1998) 187–268, https://doi.org/10.1016/S0927-796X(97)00018-1.

[20] M.A. Morris, Dislocation configurations in two-phase Ti–Al alloys III. Mechanisms producing anomalous flow stress dependence on temperature, Philos. Mag. A Phys. Condens. Matter, Struct. Defects Mech. Prop. 69 (1994) 129–150, https://doi.org/10.1080/01418619408242214.